Towards a Plasma Wake-field Acceleration-based Linear Collider*

J. Rosenzweig, N. Barov, A. Murokh

Dept. of Physics and Astronomy, UCLA

405 Hilgard Ave., Los Angeles, CA 90095-1547

E. Colby, P. Colestock

Fermi National Accelerator Laboratoryc

P.O. Box 500, Batavia, IL 60510

ABSTRACT

A proposal for a linear collider based on an advanced accelerator scheme, plasma wake-field acceleration in the extremely nonlinear regime, is discussed. In this regime, many of the drawbacks associated with preservation of beam quality during acceleration in plasma are mitigated. The scaling of all beam and wake parameters with respect to plasma wavelength is examined. Experimental progress towards high-gradient acceleration in this scheme is reviewed. We then examine a linear collider based on staging of many modules of plasma wake-field accelerator, all driven by a high average current, pulse compressed, rf photoinjector-fed linac. Issues of beam loading, efficiency, optimized stage length, and power efficiency are discussed. A proof-of-principle experimental test of the staging concept at the Fermilab Test Facility is discussed.

I. PLASMA WAKE-FIELD ACCELERATION

Much progress has been made in recent years in the experimental demonstration of acceleration in plasmas. The basic mechanisms for excitation of electron plasma waves which support accelerating fields has been verified, and accelerating gradients in excess of 30 GeV/m have been observed[1,2]. Despite this

*Work supported by U.S. Dept. of Energy grants DE-FG03-93ER0796, and the Alfred P. Sloan Foundation grant BR-3225.

¥Also at Fermi National Accelerator Laboratory.

progress, however, many problems concerning preservation of the beam quality during acceleration in high gradient plasma waves remain experimentally unaddressed; plasma wave fields tend to be nonuniform in their accelerating fields, and nonlinear in transverse focusing fields. It is critical, from the

- Acceleration which is dependent only on longitudinal position within the accelerating wave, and not on transverse offset. The maximum strength of the acceleration in this regime is typically larger than the so-called wave-breaking limit

$$eE_{WB} = m_e c^2 k_p \cong \sqrt{n_0(\mathrm{cm}^{-3})}\ (\mathrm{eV/cm}). \tag{1.2}$$

  As we typically have plasma densities at least in the range $n_0 \approx 10^{14}$ cm^{-3}, this implies accelerating gradients in excess of 1 GeV/m.
- Operation at high gradient at mm wavelengths, due to lower plasma densities and relativistic lengthening of the plasma oscillation period. This relatively long wavelength is an advantage for beam dynamics, and the smaller plasma density mitigates transverse emittance growth due to multiple scattering of the beam off of plasma ions.

We now review the characteristics of this regime in more detail, in order to illuminate the goals of our straw-man design and experimental program. Under the condition that the drive beam is much denser than the plasma, the plasma electrons are ejected from the beam channel, and the acceleration fields are entirely electromagnetic, implying that the acceleration must be independent of *r*, as in an *m*=0 TM mode traveling wave accelerator. This condition is implied by the phase independence of the focusing, as could be deduced by use of the Panofsky-Wenzel theorem[4].

This regime has been studied using PIC codes (both ISIS and a new code developed by one of the authors, N. Barov) and a fluid model[3]. The blowout of the plasma electrons, as well as the deviations from laminarity (where plasma electron trajectories cross) inherent in this regime, is well exhibited in the PIC code simulation shown in Figure 1. An example of the fluid code output is shown in Figure 2, which displays a typical case of PWFA in the blow-out regime, where a beam of twice the density (now moving to the left in the simulation) of the ambient plasma completely rarefies the beam channel, producing a pure ion channel and a nonlinear accelerating field. Figure 3 shows the dependences of the transverse and longitudinal wake-fields as a function of radius in the accelerating (for electrons) portion of the wave. It can be seen that the fields are indeed of the form discussed above, with linear focusing no transverse dependence on the accelerating field, promising great improvements in beam quality over plasma

beatwave, laser wake-field or PWFA in the linear regime. This is the relevant point, which bears repeating, that the accelerating and focusing fields in this regime are conceptually identical to a conventional linac with an applied linear focusing lattice.

The linearity of the focusing is, as stated before, due to the total rarefaction of the plasma electrons from the beam channel. This also implies other useful aspects of this system, in that beam loading within the rarefaction channel cannot change the transverse focusing. Although the blow-out regime of the PWFA has significant differences with respect to the linear regime, it also retains some advantageous aspects of the linear behavior. Most notably, ramping of the drive beam on a scale length longer than k_p^{-1} allows for a transformer ratio in excess of unity. The fact that the approximately linearly ramped pulse gives this behavior in the blowout as well as linear regimes merely reflects the degree to which the plasma response can be viewed as a generalized inductance. In this view, the decelerating field inside is nearly constant $E \propto L(dI/dt)$, which is the condition found for optimum transformer ratio generation[5].

All of the field characteristics discussed so far concern the quality of the wake-fields in the rarefaction region, where the high quality accelerating beam must be located. The transverse wake-fields for the drive beam, however, are not so uniform, because the plasma must take a finite time to respond to the beam. Because of this, the leading edge of the beam expands as if it were (ignoring small Coulomb scattering effects) in free space. On the other hand, the main body of the drive beam can be stably matched to the uniform focusing of the electron-rarefied ion channel. If the beam density is high enough, and the emittance is low, then the erosion of the beam head is not an important effect in our experimental parameterregime.

We have explored this question in great detail, with the results applied to our experimental situation and published for general use[6]. The paper presents an analytical model of how rarefaction must proceed, assuming the entire beam is in fact matched to the ion channel focusing. Given the constraint that the length of a symmetric beam must satisfy $k_p\sigma_z < 2$ (or else the wake-field behind the beam is diminished, a point which will be returned to below) the condition that the plasma electrons be rarefied before the arrival of the longitudinal beam center yields the constraint on the beam parameters,

This condition can be satisfied by a high quality rf photoinjector[7-10]. It is, however, a bit of an optimistic model, as beam-head erosion modifies this result. We have studied the effects of beam head erosion, as well as finite plasma density rise length with (1) Maxwell-Vlasov beam/plasma electron fluid computational mode, (2) superparticle beam/plasma electron fluid computational model, and (3) a fully self-consistent PIC code.

These studies have had a direct impact on experimental design and data interpretation. The most fundamental finding was that, while the scaling of Eq. 1.3 with emittance and energy is correct, the constant of proportionality is much larger, due to beam-head erosion effects. These results imply that one needs approximately a factor of 5 larger charge to achieve rarefaction.

The work performed by our group concerned the monopole stability (confinement) of the drive beam. It was thought several years ago that a dipole mode (the electron hose instability[11]) would cause problems for this type of PWFA, but it has been shown in 3-D simulations of short ($k_p\sigma_z < 2$), symmetric beams, that the instability has a negligibly small effect[12]. For long, ramped pulses, electron hose remains a serious concern.

As a final comment on the physical mechanisms in the nonlinear PWFA, we compare it (favorably) to similar schemes using laser drivers. In laser-based schemes, the laser needed is at the state of the art, especially when one considers the repetition rate, which lasers have serious limitations on due to material heating. It is also certain that the cost of a modular, staged accelerator is at present larger for the laser approach; an inexpensive approach to the PWFA is outlined in the next section. And, perhaps most critically, electron beam-based wake-field accelerators are easily phase-locked; when one uses the same rf wave and compressor to create both the drive beam and witness beam, both beams will be well-locked to the rf clock[13].

II. SCALING OF PARAMETERS IN PLASMA WAKE-FIELD ACCELERATION

The Maxwell equations, which govern the electromagnetic response of the beam-plasma system, have the property that they can be straightforwardly scaled[14]. While the detailed derivation of this scaling for the plasma wake-field system are beyond the scope of the present paper, it is possible to heuristically discuss the physics.

The object of scaling is to take a system with one or more free parameters and, once the response of the system is established, accurately predict the system response as a parameter is varied. Just as in previous work on the relativistic electrodynamics of rf photoinjectors, this scaling can be applied to two parameters: (1) the wavelength of the system, and (2) the driving beam charge $Q = -eN_b$. Because of the nonlinearity of the system under study, we must be careful to delineate how these two scaling parameters interact with each other. In order to do so we must refer first to linear theory.

One of the well known predictions of linear theory, is that the wavenumber of the excited plasma wake waves is given by the plasma density $k_p = \sqrt{4\pi e^2 n_0 / m_e v_b^2} \cong \sqrt{4\pi r_e n_0}$. It is fortunate that this result is not strongly modified by the presence of nonlinearities, which tend to diminish k_p through relativistic mass increase of the plasma electrons, even those as severe as the found in the blow-out regime. In fact the degree of nonlinearity can be considered as a form factor, dependent on the geometric ratios of the beam sizes to the plasma wavelength, $k_p\sigma_r$ and $k_p\sigma_z$, as well as the drive beam charge, or implicitly, the beam density. In order to access the blowout regime, these quantities are constrained by (1) $k_p\sigma_r << 1$, so that the plasma electrons are driven mainly radially and the impedance of the plasma is mainly inductive, (2) $k_p\sigma_z < 2$, so that the wake excitation of the wave is impulsive, allowing no significant time for the plasma to respond during beam passage, maximizing the wake amplitude, and (3) the beam density exceeds the plasma density $n_b > n_0$ (in practice the beam density must exceed this requirement by a factor of two or more).

Under the condition of constant $k_p\sigma_r$, $k_p\sigma_z$ and n_b / n_0, with the additional constraint that the form of the beam density distribution (*e.g.* Gaussian in both r and z) is held constant, the following scaling rules rigorously hold: redundantly, the assumed geometrical scaling $\sigma_r \propto k_p^{-1}$, $\sigma_z \propto k_p^{-1}$, and the scaling of beam charge $N_b \propto k_p^{-1}$ (a trivial result from the geometric requirements and constant n_b / n_0).

In order to illustrate the dependence of wake-field amplitude as a function of the plasma wavenumber and beam charge scaling parameters, it is useful to view the deceleration as a generalized *coherent* Cerenkov interaction. In this case, we can write the maximum plasma wave field ampliitude approximately as[15]

$$\left|eE_z\right| \cong N_b e^2 k_p^2 \propto k_p . \tag{2.1}$$

This expression can alternatively be trivially derived by noting equating the stored energy per unit length in the plasma wave (of transverse area $\sim \pi k_p^{-2}$) to the energy loss per unit length in the drive beam[16]. Equation 2.1 nicely displays the scaling of the wave-breaking field given in Eq. 1.2, gives an interesting result, that the field is inversely proportional to the plasma wavelength $\lambda_p = 2\pi / k_p$, and proportional to the charge, which is in turn proportional to λ_p. Thus, high gradients imply small wavelengths, which ultimately present beam handling difficulties, and *small* charges.

If we keep the beam dimensions and plasma density constant and vary the beam charge N_b, then we note, in the limit where Eq. 2.1 applies (where one can ignore small changes in k_p), that the wake-field amplitude is proportional to the plasma density (k_p^2). Also in this limit, Eq. 2.1 dictates the standard linear coherent response, that the wake-field is proportional to N_b, while the total beam energy loss rate $dU_b / dz = N_b \left\langle eE_z \right\rangle \propto N_b^2$.

III. EXPERIMENTAL WORK TO DATE

The initial tests of the plasma wake-field accelerator in the regime where $n_b < n_0$ were performed at

- Measurement of >10 MeV/m moderately nonlinear plasma waves[18].
- Time-resolved imaging of self-focused electron beam at end of plasma[19].

Additional experiments of note in this area are thin lens focusing experiments in the $n_b < n_0$ regime performed at KEK[20] and UCLA[21].

Based on the success of the initial tests at ANL, the promising theoretical predictions concerning the blow-out regime of the PWFA, and the existence of a new rf photoinjector at ANL, the Argonne Wake-field Accelerator (AWA)[22], a new collaboration was formed between UCLA and ANL to perform the next round of experiments. The initial proposal for using the AWA to generate the drive beam assumed an optimistic set of parameters: 100 nC of charge, rms bunch length of 0.75 mm, and normalized emittance of 400 mm-mrad. The predicted performance of this beam in a $n_0 = 2 \times 10^{14}$ cm^{-3} plasma ($k_p \sigma_z \cong 2$) gives a robust blowout ($n_b / n_0 \approx 8$), and a gradient of nearly 2 GeV/m. The actual performance of these experiments, which began over two years ago, have deviated considerably from these predictions, because the beam performance has been degraded in all parameters given above, and blow-out has not been straightforward to achieve. Nevertheless, the following was observed:

- Creation of a stable drive and witness beam pair in a single rf photoinjector[23].
- Deceleration of the drive beam and acceleration of the witness beam at the 10-20 MeV/m level[23].
- Time-resolved, beta-matched drive beam guiding with $n_b > 2.5 n_0$ [24].

The acceleration and deceleration were observed during the commissioning of the AWA, with somewhat derated parameters, *i.e.* $Q \approx 14$ nC and $\sigma_z \cong 3$ mm in the drive beam. The estimated wake-field, obtained from the scaling given in Eq. 2.1 along with the requirement that $k_p \propto \sigma_z^{-1}$ in this case is derated by a factor of 7 due to missing charge, and 16 due to bunch length. Thus 2 GeV/m scales to around 17 MeV/m, in accordance with observation.

Before continuing with the measurement of the wake-field acceleration under these circumstances, it was realized that the charge to emittance ratio was low enough to threaten the condition (Eq. 1.3) for obtaining the underdense condition. Because of this, and in order to more fully develop our diagnostics and understanding of the blow-out process, a series of measurements were undertaken to characterize the

focusing effects on the drive beam alone. These are reported in detail in Ref. [24]; a short discussion of the most recent results is given here.

The experimental setup for the measurement is shown in Figure 4. Electron pulses at 14.5 MeV derived from the AWA are injected from the left into the plasma chamber. Beam diagnostics immediately upstream of the plasma chamber include an energy spectrometer, an emittance measurement system, an integrating current transformer (ICT) and Faraday cup to measure Q, a phosphor screen and, at the focal point of the β-matching solenoid, an optical transition radiation (OTR) screen to obtain transverse beam profile images. The bunch length is measured using a Cerenkov radiation-based diagnostic at the end of the plasma, as described below. The plasma is created by a DC hollow cathode arc discharge with plasma density in the region of $n_0 = 1.15 \times 10^{13}$ cm^{-3}.

The plasma focusing experiments demand that Q be measured for every shot using the nondestructive integrating current transformer (ICT). The initial focal spot size near the waist of the β-matching solenoid was measured with plasma off at the OTR screen at FC1. The initial beam distribution was fit to a symmetric Gaussian with $\sigma_x = \sigma_y = \sigma_r$, with σ_r=284 ±24 μm. Using this image data, along

beam width defined by the region containing half the integrated intensity ($-x_{1/2} \le x \le x_{1/2}$) were determined. To overcome the inherent noisiness of fast streak images, 10 images within narrow input charge window ($10.2 < Q < 11.8$ nC) were summed to produce a composite picture of the beam distribution, shown in Fig. 5, along with the accompanying rms error and PIC simulation results, analyzed to give beam width as a function of *t*-slice. The experimental data and PIC simulations clearly display a profile flared at the beam head due to radial expansion, as well as a beam core which is nearly matched albeit slightly larger, $\sigma_r \cong 370\ \mu$m, due to adiabatic anti-damping of the emittance, than at input. The simulation's agreement with the data is quite good, with a notable deviation in that the experimental results generally show less pronounced beam-head expansion. The larger expansion in the simulated beam-head behavior may be due to the assumption of an input beam with a thermal transverse phase space, which is not strictly correct for a photoinjector-derived beams, where the emittance of a single *t*-slice has a smaller emittance than the full beam, with much of the total emittance arising from a longitudinal correlation of the orientation of the transverse phase space distribution[10,25]. A final comment on the time-resolved measurements is that the centroids of the beam *t*-slices displayed no significant evidence for onset of electron-hose instability.

Advances in the performance and operational understanding of the AWA during subsequent commissioning, as well as the invaluabe experience learned from the focusing measurements, in which we have established the ability to access and diagnose the blow-out regime, have allowed us to proceed to the next round of plasma wake-field acceleration experiments. These presently on-going measurements should allow us to definitively show acceleration in the blow-out regime.

IV. STAGED PWFA — A COLLIDER MODEL

Given the promise that the nonlinear PWFA shows in terms of both preservation of beam quality and achieving high gradient acceleration at moderately short wavelength, it is reasonable to ask whether this type of acceleration mechanism is appropriate for high energy physics colliders. We will therefore consider in this section a set of "straw-man" designs for a collider based on the nonlinear PWFA. This exercise will point out the issues that must be addressed in a proof-of-principle staging experiment, as well as further development of this acceleration technique.

One limitation of this technique for creating an electron-positron collider is apparent from the beginning — that positrons are not easily accelerated in the blow-out regime of the PWFA. We are thus by definition considering alternative schemes such as *e-e, e-γ* or *γ-γ* colliders, which in any event are presently subject of a fair amount of interest in the high-energy physics and accelerator communities. These considerations are not within the range of discussion here, however, and we will therefore present the collider design from the accelerator point of view, leaving the details of the interaction region purposely vague.

It was originally pointed out by W. Gai[26] that one could mitigate concerns about the transformer ratio of wake-field accelerators by driving a large number of wake-field modules from one work-horse linac. A schematic of a variation on this "hardware transformer" is shown in Figure 6. The single linac which feeds both sides of the collider must then have as many bunches in a single rf fill as the total number of modules, and in this geometry, they must be separated by the time-of-flight through a single module section, including drift. This heavily beam-loaded linac is fed by an rf photoinjector employing one or more magnetic compressors. The separate wake modules are driven by the beams, which are fanned out in a binary rf splitting scheme which is driven at the half-sub-harmonic of the linac rf frequency. These drive bunches must also be combined with the accelerating bunch, which because it will be over a TeV in energy at peak, must not see bend fields or they will lose large amounts of energy through synchrotron radiation. Thus the recombining sections must also be based on (very high frequency ~ 50 GHz) rf kickers. The stability of these rf splitting and combining systems is of course critical in determining the performance of the collider, the equivalent technical issue as timing jitter stabilization in laser-drivenaccelerators.

The parameters of the driver linac will be given for two different likely choices of rf wavelength. The parameters in the linacs are generally related by the simple scaling laws that apply to the PWFA given in Section II, with the exception of the shunt impedance and power usage. These quantities have to do with equilibrium between wall losses and resonant drive power, and are therefore not relevant to a shock-excited system like the PWFA. Despite this small difference in the type of accelerator between the drive linac and the wake-field accelerator, the scaling of parameters with respect to acceleration wavelength is a valuable tool. It should be noted that we explicitly employ this (rigorous) scaling in the designs discussed below. It is particularly notable that the use of a shorter rf wavelength in the drive linac will be taken to

imply proportionately smaller charge per bunch, bunch length, emittance and plasma wavelength in the wake-fieldaccelerator.

The first quantitative step in constructing a straw-man design is to self-consistently determine the length of a module, by setting the decelerating gradient of the beam in the module, and the energy of the beam exiting the drive linac. The decelerating gradient is of course dependent on the beam charge, emittance, bunch length and plasma density. These parameters are determined by simulation of the plasma wake-field interaction, as discussed in a following section, and are given in Table 1. Once the decelerating gradient is chosen, the accelerating gradient and plasma wavelength are also known; it remains to choose the length of the module, which sets the linac energy, as we will take the length of the module to be such that the trailing edge of the drive beam loses 95% of its energy in the plasma. The energy in turn is chosen partially by geometric considerations and partially by beam-loading considerations, the results of which are displayed in Table 2. Note that the stored energy per pulse is quite large, 60 J in the L-band case. This compares quite favorably with laser sources of similar repetition rates.

The length of the intermodule drift in the collider is chosen to give sufficient space to bring in a new drive beam and remove the spent one, match the accelerating beam optics from one module to the next, but keeping the dead (non-accelerating) space to a minimum. The total accelerating module plus dead space length is finally chosen to be commensurate with a subharmonic of the drive linac rf wavelength.

Table 2 shows a set of design parameters for the heavily beam-loaded drive linac based on a normal conducting TESLA-like L-band 1300 MHz structure, as well as a structures scaled from this design to another likely frequency in S-band, 2856 MHz; by heavily beam-loaded, we mean that the beam power absorbed from the rf power drive is well in excess of wall-dissipated rf power. The accelerating gradient is chosen to be relatively low, 6 MeV/m in the L-band case (13 MeV/m in the S-band case), in order to mitigate the rf power dissipation and related issues. These issues in this case include the peak and average power per cavity at the chosen 5% duty cycle; the peak power of 5.9 MW (8.9 MW) at a pulse length of 14.5 μsec (6.6 μsec) is easily achievable. In these designs, the majority, 78% (72%), of this power goes into accelerating the drive bunches, and the power feed profile in time is not dissimilar to TESLA, a heavily beam-loaded accelerator with higher Q values and longer time scales involved in its operation. The nominal average dissipated rf power in the L-band case is 66 kW, which is a similar power to the TTF photoinjector power[27], but with nearly an order of magnitude more total mass. Similarly, the

S-band cavities have much less power density to handle than the Grumman high-duty cycle gun. The cooling of the rf cavities should therefore be a straightforward design problem.

Since, unlike standard rf linac based colliders, multi-bunching is not possible, the rf pulse rate (and duty cycle) are quite high, in the MHz range, as is necessary for high luminosity. This pulse rate is limited in general by the previously mentioned cooling considerations, which must also be examined for the rf sources as well as the linacs. The general philosophy adopted here for the accelerating beam is to put as much particle flux into the interaction region as possible. The development of coherent instabilities (*i.e.* beam-breakup) in the wake-field accelerator itself, as well as in the drive beam linac, will undoubtedly be the limiting factor in how much charge can be accelerated in this scheme. We have chosen the parameters here only on the basis of power and energy considerations, to obtain values of N_b and collision rate f_{rep} (see below) close to those of conventional collider designs. Discussion of higher order effects which may interfere with achieving these goals must await future work.

Table 3 shows the parameters associated with the accelerated beam and the total system performance. The efficiency of energy extraction from the wake is kept to 20%, in order to load the beam at 91% of the peak amplitude (transformer ratio of approximately 1.8 per module). This gives a center-of-mass energy at the collision point of 2.5 TeV, with collisions occurring at an average rate of f_{rep} = 3.5 kHz. Assuming a wall-plug efficiency associated with the 1300 MHz rf system of 50%, we obtain an average power of 270 MW to run the collider. This is within the range of acceptable powers for this type of third-generation (post-NLC) collider. The total power efficiency, which is somewhat dependent on the value of $k_p\sigma_z$ through the ratio of average-to-peak energy loss in the drive bunch, is in the range of 5% for both designs.

Although a discussion of scaling and luminosity is included in the following section, no luminosity estimates will be attempted at this point, as there are many issues associated with the emittance dynamics in the collider, as well as the detailed design of the (γ - γ, e^- - γ or e^--e^-) collider final focus and interaction point. The interaction point is again a complex subject well beyond the scope of present consideration; let us now examine only the relevant issue of emittance.

There are two fundamental physical mechanisms which give rise to emittance variation in this type of accelerator - emittance damping due to dipole radiative decay of the betatron oscillation amplitude, and emittance growth due to multiple scattering off of the plasma ions. Of course, there are many other

sources of emittance growth, including higher focusing multipole moments, chromatic and collective transverse instability. The damping of oscillations in a uniform focusing channel such as the plasma ion-focusing column we are considering has been analyzed in detail by Huang, Chen and Ruth[28]. The equation for emittance damping derivable from this work is

$$\frac{d\varepsilon_n^2}{dz} = -\frac{2\pi r_e^2 n_0}{3}\varepsilon_n^2, \tag{3.1}$$

which yields exponential damping with characteristic length $z_d = 3/2\pi r_e^2 n_0$. For the plasma densities of interest here this damping length is enormous, on the order of 10^8 m, and thus we can ignore this effect henceforth; only in the case of a nearly solid state plasma density would this effect be strong enough to consider.

On the other hand, the excitation of the emittance growth due to multiple scattering can be quantified by the following expression, based on the familiar angular growth formula due to Bethe,

$$\frac{d\varepsilon_n^2}{dz} \cong 9.13\left(\frac{n_0 r_e^3}{\gamma}\right)^{1/2}\frac{Z^2\ln\left(184/Z^{1/3}\right)}{A}\varepsilon_n. \tag{3.2}$$

This can be integrated, assuming small emittance growth,

$$\Delta\varepsilon_n^2 \cong 18.25\left(n_0 r_e^3\gamma_f\right)^{1/2}\frac{Z^2\ln\left(184/Z^{1/3}\right)}{A}\frac{\varepsilon_n m_e c^2}{eE_{acc}}. \tag{3.2}$$

For the parameters of this collider design the rms normalized emittance increase, assuming a hydrogen plasma and beginning with an rms normalized emittance of $\varepsilon_n = 10^{-8}$ m-rad (the vertical emittance from a state of the art damping ring), is $\sqrt{\Delta\varepsilon_n^2} \cong 1.33\times10^{-9}$ m-rad, consistent with the assumption of small growth. This, along with the particle fluxes given above, indicate that a plasma wake-field accelerator based linear collider merits further consideration.

It should be noted at this point that the laser-driven variations on plasma acceleration, generally demand a higher plasma density in order to guide the laser, in analogy to the ion-focusing considered here.

This is because the effective emittance of the laser beam, $\varepsilon_l = \lambda_l / 4\pi$, is much larger than that of the mult-MeV electron beam considered in our straw-man design. The laser divergence must be controlled by a

IV. PROPOSED EXPERIMENTAL PROGRAM: STAGING

A state-of-the-art, high charge, low emittance 1300 MHz rf photoinjector, with chicane compressor[13], termed the Fermilab Test Facility[27], is now under construction at Fermilab. This injector is a prototype for the TESLA Test Facility Injector to be installed in 1998 at DESY, and also will serve as a test bed for research into new ideas in particle beam physics. Among the formally proposed experiments is a collaboration (FNAL P890) between UCLA, Univ. of Rochester, and FNAL, to perform a first test of staging in plasma accelerators. It should also be noted that this configuration of the photoinjector and compressor is close to a scaled version of the S-band photoinjector/compressor presently being commissioned in the Neptune Laboratory[29] at UCLA.

The prediction of the wake-field amplitude driven by a 20 nC, 0.8 mm bunch length beam in a $n_0 = 10^{14}\,\mathrm{cm}^{-3}$ plasma, obtained by PIC simulation, with the initial particle distribution derived from PARMELA, is approximately 1 GeV/m. These simulations serve to verify the wake-field amplitude used in the above straw-man design, which uses nearly identical parameters. The importance of this experimental test is that it, along with experiments planned for the Neptune photoinjector[29], will be the first wake-field experiments using a compressor. These two tests, performed at two different rf wavelengths, will also allow two points along the road to scaling down in wavelength to be obtained. This march towards higher gradient with shorter beams should be continued at SLAC with the FFTB PWFA experiment[30].

In addition, the FNAL experiments are proposed to demonstrate the stageablity of this PWFA scheme. Figure 7 shows a schematic of the proposed configuration for a two-stage PWFA experiment at the FTF. Two sets of witness and drive beams are split by use of a one-half subharmonic deflection mode cavity. The first witness beam is accelerated in the initial stage, and is then reinjected into the second stage for further acceleration. This experiment will be technically quite challenging, pushing ever further our abilities to handle beams with smaller physical dimensions, techniques which will be necessary for future high energy physics accelerators.

REFERENCES

1. K. Nakajima, *et al., Phys. Rev. Lett.* **74**, 4428 (1995).
2. C.E. Clayton, *et al., Phys. Rev. Lett.* **70**, 37 (1993).
3. J.B.Rosenzweig, *et al.*, *Phys.Rev.A* **44**, R6189 (1991)
4. W. K. H. Panofsky and W. A. Wenzel, *Rev. Sci. Inst.* **27,** 967 (1956).
5. K.Bane, *et al., IEEE Trans. Nucl. Sci* **32**, 3524 (1985)
6. N. Barov and J.B. Rosenzweig, *Phys. Rev. E* **49** 4407 (1994).
7. J.S. Fraser, *et al., IEEE Trans. Nucl. Sci.* **NS-32**, 1791 (1985).
8. B.E. Carlsten, *Nucl. Instr. Methods A* **285**, 313 (1989).
9. C. Travier, *Particle Accelerators* **36**, 33 (1991).
10. Luca Serafini and James B. Rosenzweig, *Phys. Rev. E* **55**, 7565 (1997).
11. D. Whittum, *et al., Phys. Rev. Lett.* **67** (1991).
12. J. Krall and G. Joyce, *Advanced Accel. Concepts* 505 (AIP Conf. Proc. 335, 1995).
13. J.B. Rosenzweig, N. Barov and E. Colby, *IEEE Trans. Plasma Sci.* **24**, 409 (1996).
14. J.B. Rosenzweig and E. Colby, *Advanced Accelerator Concepts*, **335**, 724 (AIP Conf. Proc., 1995).
15. J.D. Jackson, *Classical Electrodynamics* (Wiley,1975).
16. A. Ogata, *et al.,* these proceedings.
17. J.B.Rosenzweig, *et al., Phys.Rev.Lett.* **61**, 98 (1988).
18. J.B. Rosenzweig, *et al., Phys.Rev.A* **39**, R1586 (1989).
19. J.B. Rosenzweig, *et al., Phys. Fluids B* **2**, 1376 (1990).
20. H. Nakanishi, *et al., Phys.Rev.Lett.* **66**, 177 (1991).
21. G.Hairapetian, *et al. Phys.Rev.Lett.* **72**, (1994).
22. P. Schoessow, *et al., Proc. 1995 Particle Accelerator Conference,* 976 (IEEE, 1996).
23. N. Barov, *et al., Proc. 1995 Particle Accelerator Conference,* 631 (IEEE, 1995).
24. N. Barov, *et al.,* submitted to *Phys. Rev. Lett.* (1997).
25. 16. X. Qiu, *et al.*, *Phys.Rev.Lett.* **76**, 3723 (1996).
26. W. Gai, *Advanced Accel. Concepts,* **340** (AIP Conf. Proc., 1990).
27. E. Colby, *et al. Proc. 1995 Particle Accelerator Conference,* 1445 (IEEE, 1995).
28. Z. Huang, *et al. Phys. Rev. Lett.* (1996).
29. J.B. Rosenzweig, *et al.,* these proceedings.
30. R. Assman, *et al.,* these proceedings.

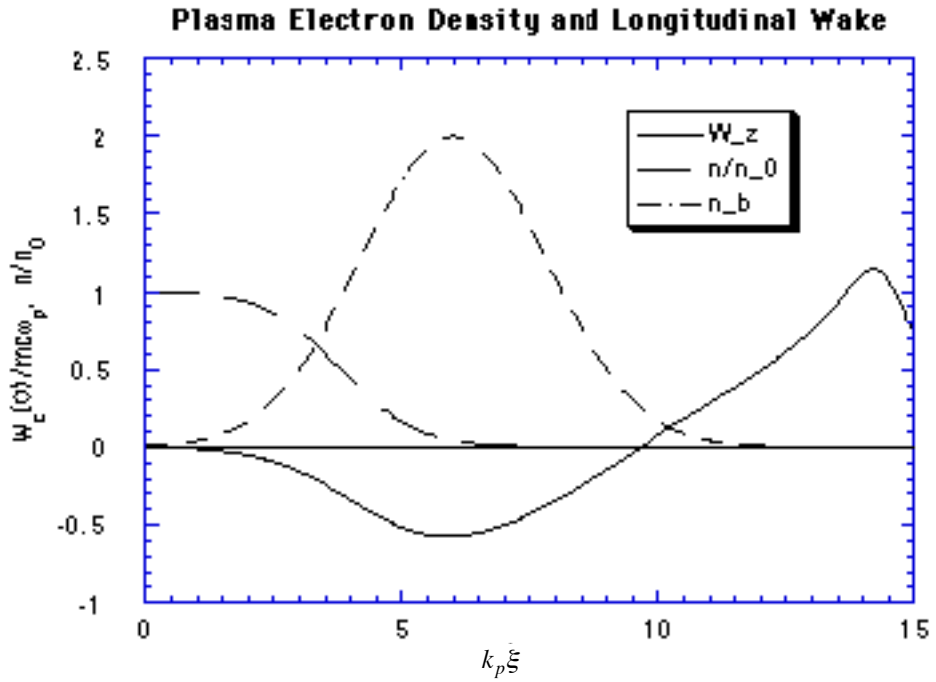

Figure 2. PWFA in the blow-out regime, beam completely rarefies plasma electrons from the beam channel. Longitudinal coordinate is stationary within the wave $\xi \equiv v_b t - z$.

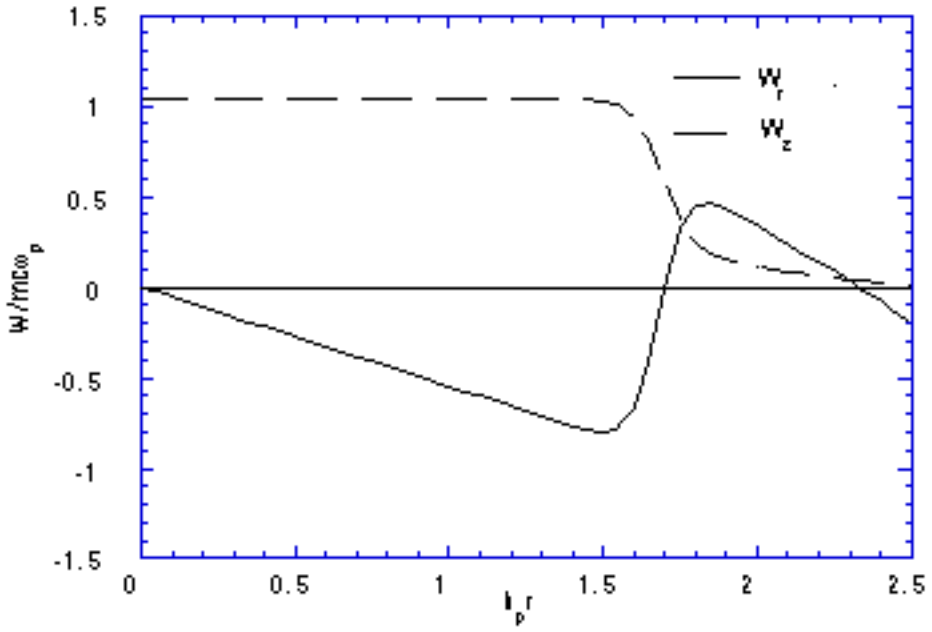

Figure 3 . Transverse and accelerating fields as a function of radius at accelerating phase of case in Figure 2, showing uniform acceleration, linear focusing within rarefaction channel.

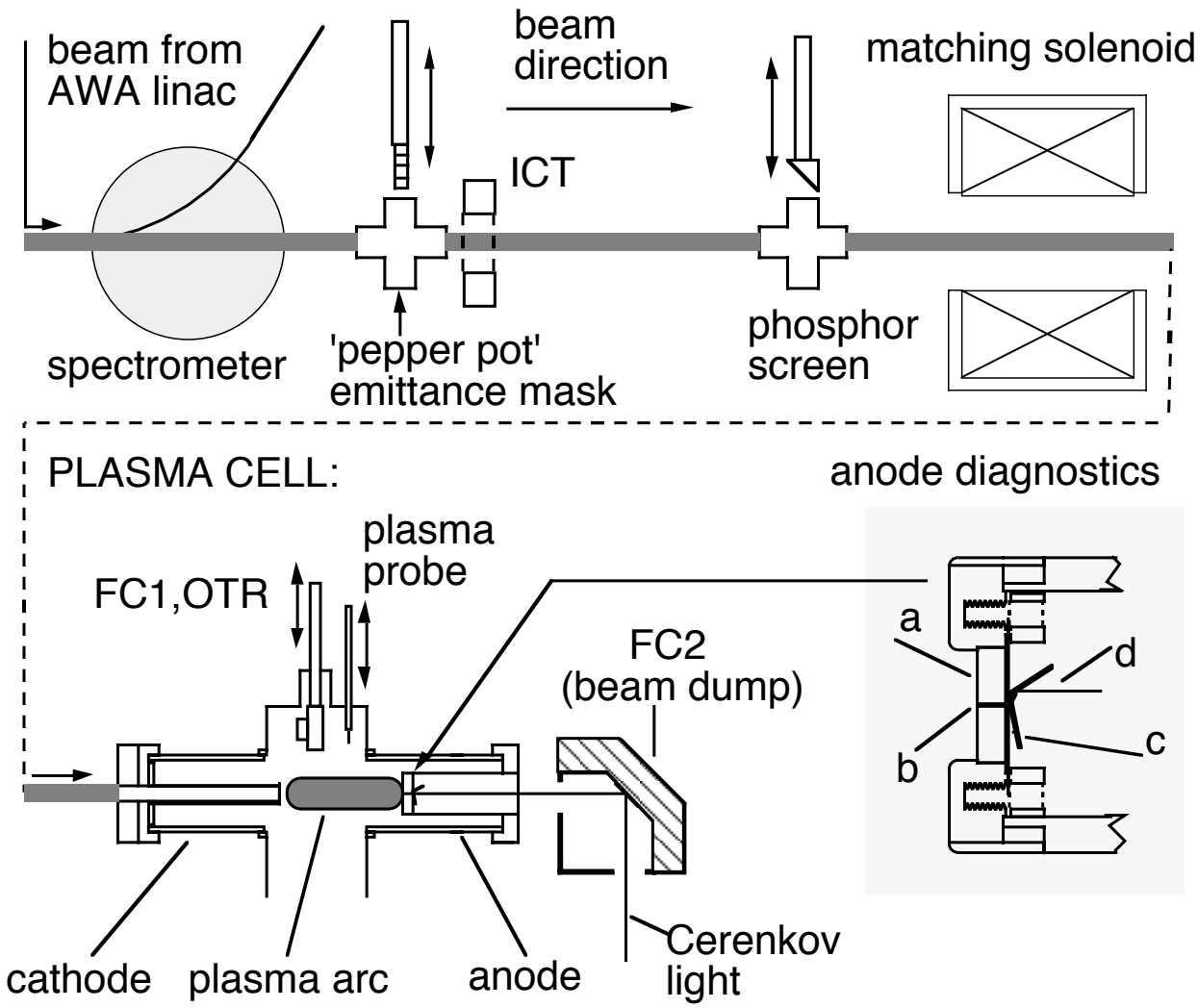

Figure 4. Diagnostics beamline and plasma cell (shown without the plasma radial confinement solenoid). The anode diagnostics include (a) tungsten collimator with (b) 1 mm wide slit, (c) 500 μm thick quartz Cerenkov radiator, and (d) mirror and outgoing light.

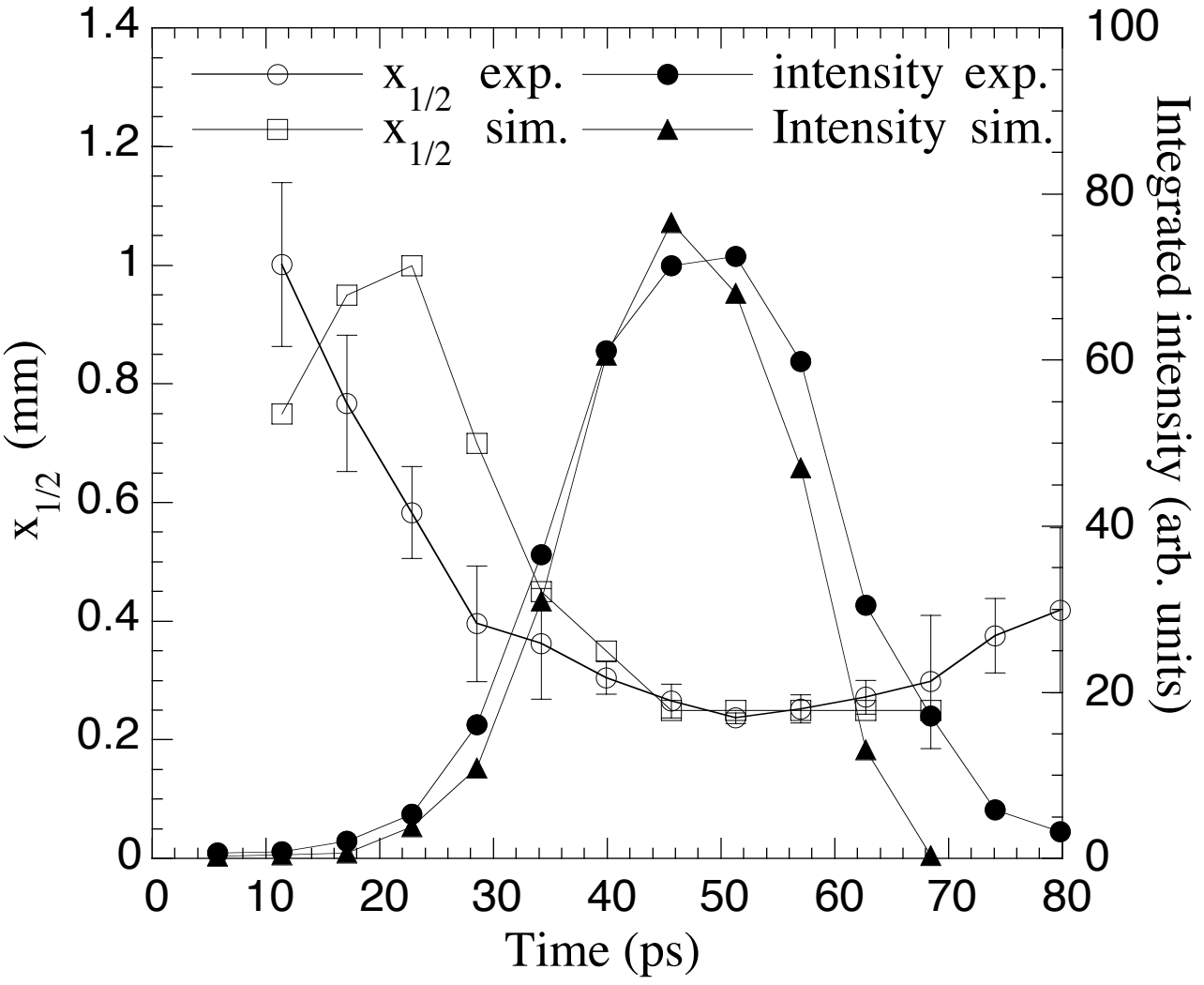

Figure 5. Time-slice dependence of beam intensity and half-width, from experiment (exp.) and PIC simulation (sim.).

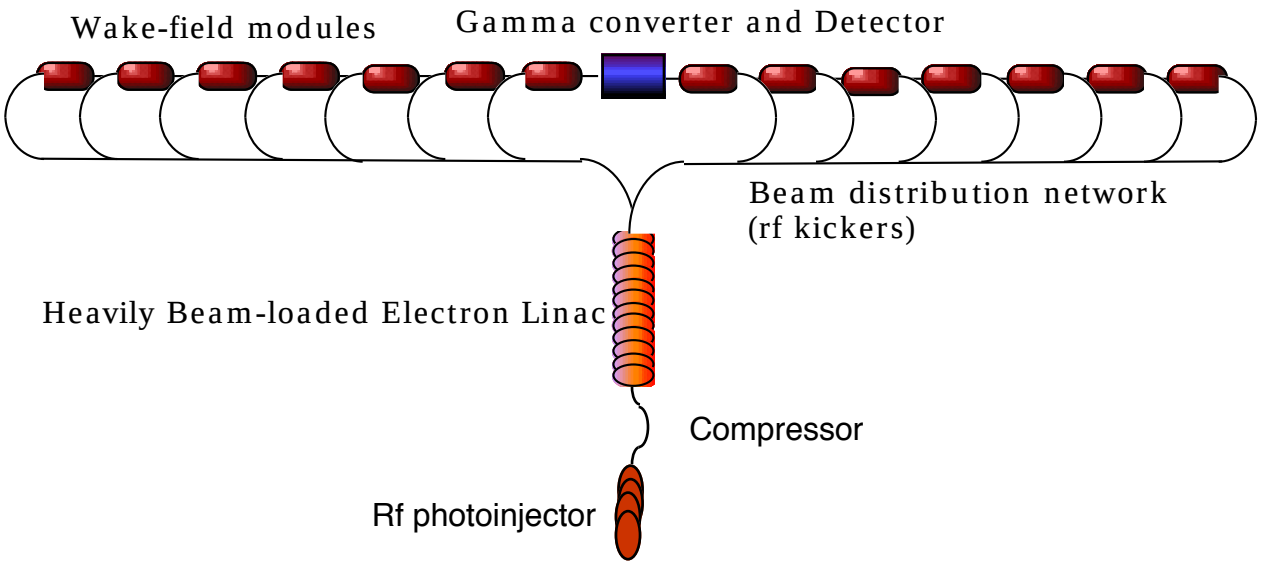

Figure 6. Schematic of a γ–γ collider using a hardware transformer scheme. A large number of bunches are created in heavily beam-loaded linac fed by an rf photoinjector followed by a compressor. Separate wake modules are driven by the beams, which are fanned out in a binary rf splitting scheme.

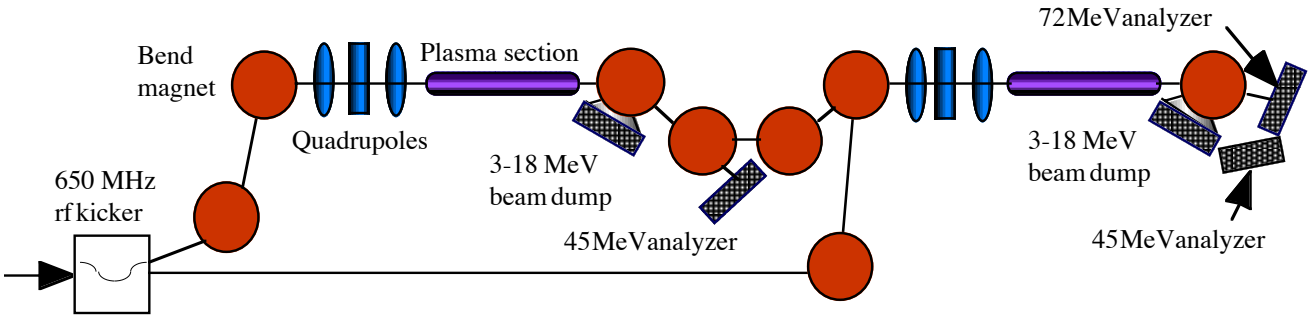

Figure 7. Schematic of two-module plasma wake-field experiment, with rf splitter, two plasma sections, combining optics, beam dumps and energy analyzers shown. Not shown: emittance, pulse length diagnostics.

TABLE 1. Nominal drive beam and accelerating module parameters for the plasma wake-field accelerator-based collider shown in Figure 4.

	L-band case	S-band case
Beam Energy	3 GeV	3 GeV
Beam Charge	20 nC	9 nC
Stored Energy/Bunch	60 J	27 J
Bunch Length	0.8 mm	0.36 mm
Norm. Emittance	50 mm-mrad	23 mm-mrad
Plasma Density	2×10^{14} cm^{-3}	10^{15} cm^{-3}
Plasma Wavelength	2.2 mm	1 mm
Deceleration Wake	500 MeV/m	1.1 GeV/m
Accelerating Wake	1 GeV/m	2.2 GeV/m
Wake Module Length	5.7 m	2.6 m
Intermodule Drift	2.66 m	1.21 m

TABLE 2. Design parameters of heavily beam-loaded 1300 MHz drive linac for plasma wake-field collider. Parameters chosen based on Table 1 parameters, optimized for high level of beam-loading (beam power well in excess of dissipated rf power).

	L-band case	S-band case
Avg. accel. gradient	6 MeV/m	13.2 MeV/m
Shunt impedance $Z'T^2$	30 MW/m	45 MW/m
Active length	500 m	227 m
Cavity length	1.1 m	0.5 m
Peak rf power (cavity)	5.9 MW	9 MW
Number of bunches	2 x 250	2 x 250
Beam current (in fill)	690 mA	1.5 A
RF flat top	14.5 msec	6.6 msec
Duty cycle	5%	5%
Avg. bunch rep. rate	865 kHz	1.9 MHz
Avg. diss. rf power/cavity	66 kW	96 kW
Total ave. diss. RF power	30 MW	43.5 MW
Total avg. beam power	104 MW	104 MW

TABLE 3. Accelerated beam, system collider performance.

	S-band case	L-band case
Accelerated charge	2 nC	0.9 nC
Wake extraction efficiency	20%	20%
Length of Collider	2 x 2.16 km	2 x 2.16 km
Accel. beam energy	1.25 TeV	1.25 TeV
Avg. collision rate	3.5 kHz	7.7 kHz
Drive linac/wall powe effic.	50%	50%
Total wall power	270 MW	295 MW
Total efficiency	5.4%	4.9%